

1 A pyrolysis approach for characterizing and assessing 2 degradation of polyurethane foam in cultural heritage objects

3
4 Jacopo La Nasa^a, Greta Biale^a, Barbara Ferriani^{b,c}, Maria Perla Colombini, Francesca
5 Modugno^{a*}

6
7 ^aDepartment of Chemistry and Industrial Chemistry, University of Pisa, Pisa, Italy

8 ^bConservation Laboratory at the Triennale Design Museum, Milano, Italy

9 ^cBarbara Ferriani S.r.l., Milano, Italy

10 *: francesca.modugno@unipi.it

11 12 **Abstract**

13 Specific analytical tools are needed to investigate the composition and degradation processes of the
14 synthetic materials in the cultural heritage, and recent advancements in pyrolysis-based analytical
15 techniques have great potential for the characterisation of synthetic polymers. We applied evolved gas
16 analysis mass spectrometry (EGA-MS) and double shot pyrolysis coupled with chromatography and
17 mass spectrometry (Py-GC/MS) to investigate polyurethane foam micro-samples from the Italian pop-
18 art sculpture “Contentitoreumano n.1” (1968) by Ico Parisi (1916-1996) and Francesco Somaini (1926-
19 2005). The chemical analysis aimed to assess the chemical composition and of the state of
20 preservation of the PU foam by acquiring information on its thermal degradation behaviour and
21 identifying the pyrolysis products produced at different temperatures. A preliminary ATR-FTIR
22 analysis was also carried out. The multi-analytical approach enabled us to identify the isocyanate and
23 polyol precursors as 2,6-toluenediisocyanate and polypropylene glycol, respectively. The plasticizers
24 used in the production of the PU foam were also identified in the first shot of a double shot Py-GC/MS
25 experiment. A comparison of a sample of better preserved foam with a sample of degraded foam from
26 the surface of the object highlighted that the more degraded part of the PU foam featured an increase
27 in the thermal degradation temperature of the soft-fragments of the PU network, related to cross-
28 linking phenomena. Moreover, loss of plasticizers and formation of NH₂ functional groups was
29 observed in the degraded foam.

30 31 32 **Keywords**

33 Polyurethane foams, Cultural Heritage Objects, Degradation processes; Analytical Pyrolysis, Evolved
34 Gas Analysis

35

36 1. INTRODUCTION

37 The 20th century witnessed a revolution in the composition of artists' materials. Today, modern
38 and contemporary collections face challenging conservation issues related to the wide variety of
39 synthetic polymer-based plastics present in art and design collections [1,2].

40 To preserve the stability of synthetic polymeric materials, some of which were not intended to last
41 longer than a few decades after their production, specific analytical tools are required for their
42 identification, to investigate the degradation processes, and to assess the preservation state of specific
43 objects. In this context, analytical pyrolysis is emerging as a fundamental tool for the analysis of
44 polymers in heritage science [3-10], also thanks to recent developments such as evolved gas analysis
45 mass spectrometry (EGA-MS) and multi-shot pyrolysis coupled with chromatography and mass
46 spectrometry (multi-shot Py-GC/MS). These techniques have only been applied in heritage studies in a
47 few cases, but have shown a good potential in the investigation of synthetic paint binders [11-14],
48 archaeological wood [15], and conservation materials such as wood consolidants [16], lacquers [17],
49 and proteinaceous residues [18].

50 Of the synthetic polymers encountered in 20th century artworks and design objects, polyurethane was
51 first synthesized in 1937 in Germany. However, it was only in the late 1960s, as a consequence of the
52 widespread use of polyurethane in the industrial production of everyday objects, that artists
53 approached this new material attracted by its peculiar and innovative features, as lightness and
54 softness [19,20]. Polyurethanes can also be found as a constituent of works of art such as rigid and
55 flexible foams in design objects and sculptures [21]. Today conservators are faced with the limited
56 durability of polyurethane foams which affects the stability of the artworks. In fact, the first
57 polyurethanes began to degrade only a few decades after their production [20,21]. The limited
58 knowledge available on the degradation of polyurethane foams, along with the wide variety of possible
59 compositions for these materials, make the degradation of PU foams a critical conservation issue
60 [20,21].

61 Infrared spectroscopic techniques have proven efficient in characterising different classes of polymers
62 including PU [22-27].

63 However a detailed molecular analysis and the identification of specific monomeric precursors require
64 a micro-invasive characterisation of samples, which is possible by Py-GC/MS [20,28,29].

65 EGA-MS, which has shown promising results in the analysis of polyurethanes [30], and combined with
66 multi-shot Py-GC/MS has great potential in the selective characterisation of plastic components on the
67 basis of their thermal decomposition behaviour.

68 In this work, we evaluated a combination of EGA-MS and double shot Py-GC/MS in the investigation of
69 a polyurethane foam sculpture pertaining to Italian pop art, "Contentoreumano n.1" (1968) by Ico
70 Parisi (1916-1996) and Francesco Somaini (1926-2005), which is shown in Figure 1. The chemical
71 analysis of the foam constituting the object, which could be ambiguously classified both as an artwork

72 and as the prototype of a piece of design furniture, took place before a conservation intervention
73 performed by Triennale Design Museum of Milan in 2017 [31]. A preliminary ATR-FTIR analysis was
74 also carried out [8,9,32]. Micro-samples of PU foam with different states of preservation were
75 examined, in order to obtain a picture of the chemical composition and of the degradation processes of
76 the PU, based on its thermal degradation behaviour. The two pyrolysis-based approaches were applied
77 in this study for the first time in the characterisation of PU in cultural heritage.

78
79



80
81 Figure 1. The Contenitoreumano n.1 by Ico Parisi and Francesco Somaini, 1968, metal and polyurethane foam,
82 1250 x 1575 x 92 cm, in a historical photograph (left) and after the 2017 conservation intervention. Photo:
83 Triennale Design Museum (Milan).
84

85

86 2. MATERIALS AND METHODS

87 2.1 Investigated materials and samples

88 The investigated object, dated 1968, is one of the two existing prototypes of Contenitoreumano n.1 by
89 Ico Parisi and Francesco Somaini, originally consisting of a metallic case painted white with handles on
90 both sides, on which the words “Contenitoreumano” were written in red followed by the authors’
91 names. The name of the prototype series could be translated as “Human receptacle” or “Human
92 container”, and the series was intended as a utopian reflection on human inhabitation [31]. This shell
93 contained a soft internal structure created by the juxtaposition of various layers of molded
94 polyurethane foam, equipped with plastic tubes imagined delivering food and drink to the person
95 inside (Figure 1). The prototype was restored at the Conservation Laboratory of the Triennale Design
96 Museum of Milan in 2017. The sampling and analysis were carried out within the framework of the
97 IPERION CH.it project “Plastic in the collection of the Triennale Design Museum in Milan”. Micro-
98 sampling followed by laboratory analysis was selected as the investigation approach because a non-

99 invasive characterization by a portable in situ spectrophotometric technique was not possible for this
100 porous material.

101 Two fragments of polyurethane foam from the artwork were collected (around 2 mg each,
102 corresponding to few mm³ of foam): one from the bulk of the foam, identified as CU3, which appeared
103 to be less degraded, and the other fragment from the external surface of the foam, identified as CU4,
104 which showed a certain degree of yellowing, and was more rigid and brittle than the bulk material. The
105 two fragments were directly examined by ATR-FTIR, and then sub-sampled for EGA-MS and Py-GC/MS
106 micro-destructive analysis.

107

108 **2.2 Optical microscopy**

109 Optical microscopy images of the foam fragments were acquired using an Olympus BX51M optical
110 microscope equipped with fixed oculars of $\times 10$, and lenses with $\times 5$ magnification (the other possible
111 magnifications are $\times 10$, $\times 20$, $\times 50$ and $\times 100$) for dark field observations. The instrument was equipped
112 with a 100 W halogen projection lamp for visible light acquisition, and with an Olympus U-RFL-T lamp
113 for visible fluorescence acquisition. The images were recorded with a digital scanner camera Olympus
114 XC50 directly connected to the microscope.

115

116 **2.2 Attenuated total reflectance infrared spectroscopy (ATR-FTIR)**

117 ATR-FTIR spectra were collected directly on fragments of foam using a Perkin Elmer Spectrum 100
118 spectrometer coupled with a MIRacle TM ATR accessory equipped with a SeZn crystal. Sixteen scans
119 were collected from 4000 to 650 cm⁻¹ with a resolution of 4 cm⁻¹. The analyses were performed at
120 room temperature (22°C). Jasco Spectra Manager software was used for data analysis.

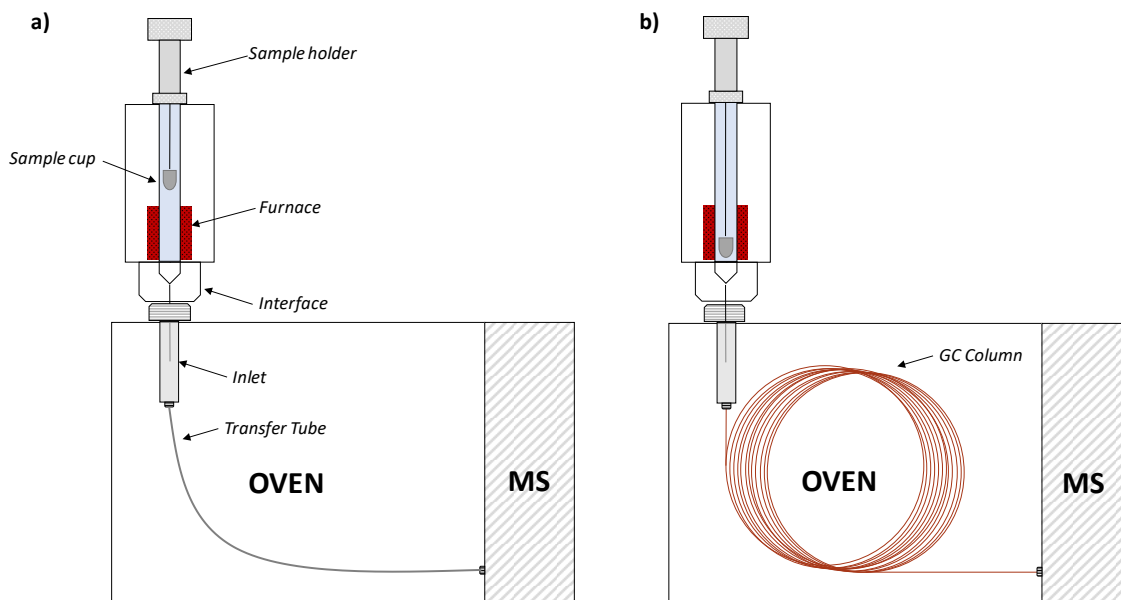
121

122 **2.3 Evolved gas analysis-mass spectrometry**

123 The samples were placed into a pyrolysis stainless-steel cup, weighted, and inserted into the
124 microfurnace. The weight of samples was CU3 and CU4 were 106 μg and 98 μg respectively. The
125 instrumentation consisted of a micro-furnace Multi-Shot Pyrolyzer EGA/Py-3030D (Frontier Lab,
126 Japan) coupled with a gas chromatograph oven 6890 Agilent Technologies (USA) kept at 300°C,
127 connected with a mass the Mass Selective Detector single quadrupole mass through an Ultra ALLOY ®
128 EGA Tube (2.5 m x 0.15 mm i.d).

129 Temperature program for the micro-furnace chamber of the pyrolyzer: initial temperature 50 °C; 10
130 °C/min up to 800 °C for 10 minutes. Analyses were performed under a helium flow (1 ml/min) with a
131 split ratio 1:20. The micro-furnace interface temperature was automatically kept at 100 °C higher than
132 the furnace temperature up to the maximum value of 300 °C. The inlet temperature was 280 °C. The
133 mass spectrometer was operated in EI positive mode (70 eV, scanning m/z 50-700). The MS transfer

134 line temperature was 300 °C. The MS ion source temperature was kept at 230 °C, and the MS
135 quadrupole temperature at 150 °C. A scheme of the analytical set-up is shown in Figure 2a.
136
137



138

139 **Figure 2** Instrumental asset of the Frontier Lab Multi-Shot Pyrolyzer EGA/Py-3030D used for a) evolved gas
140 analysis/mass spectrometry (EGA-MS) and b) multi-shot pyrolysis-gas chromatography/mass spectrometry (Py-
141 GC/MS) .

142

143 **2.4 Multi-shot pyrolysis-gas chromatography/mass spectrometry**

144 Analyses were performed using a multi-shot pyrolyzer EGA/PY-3030D (Frontier Lab) coupled with a
145 6890N gas chromatography system with a split/splitless injection port, and with a 5973 mass selective
146 single quadrupole mass spectrometer (both Agilent Technologies) [33], as shown in Figure 2b.

147 The samples were placed in stainless-steel cups and the sample weights were CU3 and CU4 were 56 µg
148 and 60 µg respectively. Multi-shot pyrolysis conditions were optimized as follows: pyrolysis
149 temperatures were selected based on the specific EGA/MS results for each sample: the first shot was
150 performed at 306°C and the second at 600°C.

151 interface 280 °C. The GC injector temperature was 280 °C. The GC injection was operated in split mode
152 with a split ratio of 1:10. The chromatographic separation of pyrolysis products was performed on a
153 fused silica capillary column HP-5MS (5% diphenyl-95% dimethyl-polysiloxane, 30 m x 0.25 mm i.d.,
154 0.25 µm film thickness, J&W Scientific, Agilent Technologies), preceded by 2 m of deactivated fused
155 silica pre-column with an internal diameter of 0.32 mm. The chromatographic conditions were: 40 °C
156 for 5 min, 10 °C/min to 310 °C for 20 min. The helium (purity 99.9995%) gas flow was set in constant
157 flow mode at 1.2 mL/min [7-9,34-36].

158 MS parameters: electron impact ionization (EI, 70 eV) in positive mode; ion source temperature 230
159 °C; scan range 50-700 m/z; interface temperature 280 °C. Perfluorotributylamine (PFTBA) was used
160 for mass spectrometer tuning. MSD ChemStation (Agilent Technologies) software was used for data

161 analysis and the peak assignment was based on a comparison with libraries of mass spectra (NIST 1.7,
162 WILEY275) and the literature data [29].

163

164

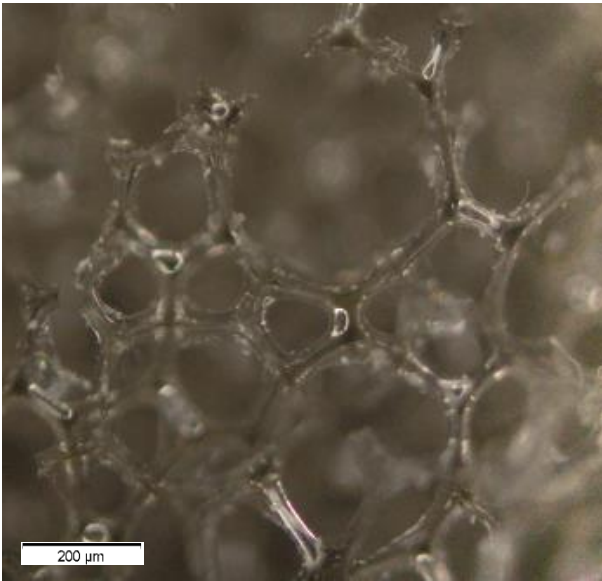

165 **3. RESULTS AND DISCUSSION**

166 **3.1 Optical microscopy**

167 The microscopic comparison of the better preserved and the more degraded samples from
168 Contenitoreumano (Table 1) showed damage of the polymeric cell-like structure in the sample CU4
169 from the surface of the object. The materials also appeared more yellow and darkened compared to
170 sample CU3. Yellowing is a significant indicator of chemical changes in polymers containing aromatic
171 structures, and it can be expected to occur as a result of the formation of additional double bonds
172 conjugated with the aromatic ring [37].

173

174 **Table 1** Investigated samples from “Contenitoreumano n.1” and optical microscopy images.

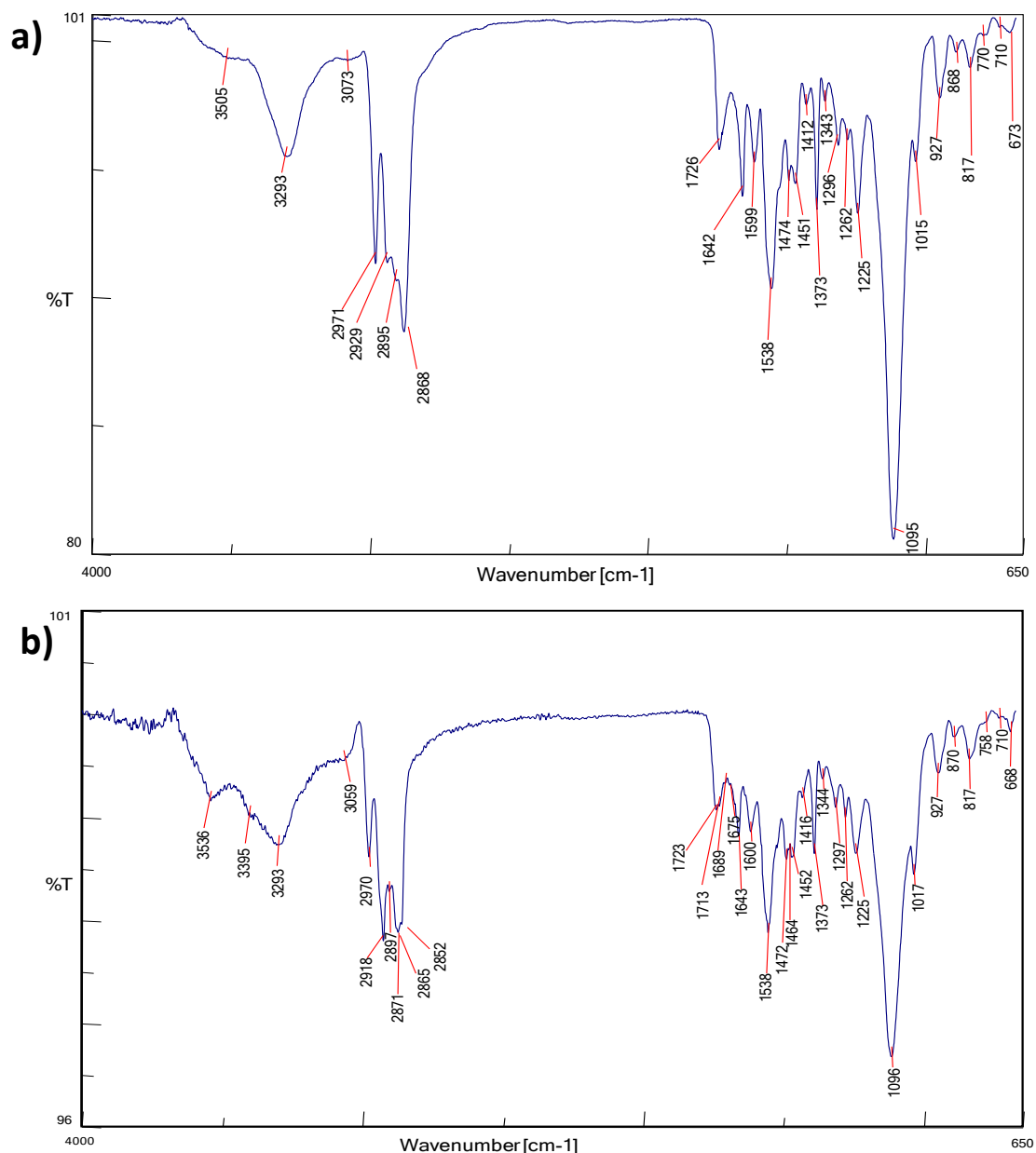
Sample	Optical microscopy
CU3 Bulk foam, better preserved	
CU4 Surface foam, significantly degraded	

175

176

177 **3.2 ATR-FTIR**

178 Figure 3 shows the ATR-FTIR spectra of samples CU3 (bulk) and CU4 (surface). The identification of
 179 the observed ATR-FTIR bands is reported in Tables 2 and 3 for samples CU3 and CU4, respectively
 180 [19,38-42].



181
 182 **Figure 3** ATR-FTIR spectra obtained for the samples: a) CU3 (bulk) and b) CU4 (surface) from
 183 “Contentioreumano n.1”. The band assignments are reported in Tables 2 and 3.
 184

185 ATR-FTIR shows that the polyurethane used in “Contentioreumano n.1” is a polyether-based
 186 polyurethane. The polyether-based polyol marker is the asymmetric stretching vibration of C-O-C at
 187 1095 cm⁻¹. PUs are also strongly self-associated through intermolecular hydrogen bonding [43]. The
 188 hydrogen bonding interactions are formed between the hard segments of the polyurethane and
 189 consist in the physical crosslink of PUR flexible foams (virtual crosslink). Studies have demonstrated
 190 that these interactions act as a covalent bonding at room temperature, and are significant in the

191 determination of PU properties [44]. The absorption bands related to hydrogen bond interactions are:
192 3661-3434 cm^{-1} (stretching vibration of non-H-bonded N-H), 3293 cm^{-1} (stretching of H-bonded N-H),
193 1723-1726 cm^{-1} (stretching vibration of non H-bonded urethane), and the carbonyl band at 1630-
194 1730 cm^{-1} . Other significant regions are between 3000 and 2850 cm^{-1} (-C-H₃ and -C-H₂ stretching) and
195 between 930 and 600 cm^{-1} , which includes the bending of C-H benzene rings and the -C-H₂ skeletal
196 deformations.

197 To highlight spectral changes related to the deterioration of the polyurethane foam, the two spectrums
198 of the better-preserved bulk sample (CU3) and the more degraded surface sample (CU4) were
199 compared. The main differences between the PU portion with different state of preservation were
200 observed evaluating the N-H, C-H and C=O (amide I) stretching regions, comparing relative intensities
201 of bands in the same spectra. The surface sample CU4 showed a changing in the relative intensity of
202 the broad band between 3661 and 3000 cm^{-1} . In this region N-H stretching vibration bands occur,
203 together with a band at approximately 3395 cm^{-1} which can be attributed to the formation of quinone-
204 imides with hydroperoxides as intermediates [45]. These products, along with the decrease in the
205 relative intensity of the C-O-C band, suggest the partial scission of the soft segment due to the
206 photooxidation process. Moreover, the photo oxidation was further confirmed by the presence of the
207 new band appearing at 3536 cm^{-1} accompanied by the decrease of relative intensity of absorption
208 band at 1642 cm^{-1} suggesting the formation of amines according to e.g. photo-Fries type of mechanism
209 in polyurethanes [46], as highlighted also by EGA-MS (Figure 5).

210 Concerning the C-H stretching region (3000-2850 cm^{-1}), the surface sample CU4 showed a reduction
211 in the band at 2970 cm^{-1} (C-H₃ asymmetric stretching) and a relatively higher intensity of the C-H₂
212 stretching absorption at 2918 cm^{-1} , in comparison to CU3. These alterations could be related to
213 reticulation processes which may occur as a consequence of the formation of reactive compounds as
214 products of the photo-oxidative degradation of polyether-based polyurethane.

215 The carbonyl region (1800-1630 cm^{-1}) is also significant in the evaluation of foam degradation: CU4
216 spectrum showed the presence of bands, which were not present in the CU3 spectrum, at 1713, 1689
217 and 1675 cm^{-1} which were identified as urethane loosely associated through H-bonds, free urea, and
218 disordered H-bond monodentate urea respectively [38,39]. The formation of free urea is the sign of
219 the cleavage of urethane bonds, while the bands at 1713 and 1675 cm^{-1} could be related to the bond
220 rearrangement due to cross-linking involving reaction of amines with urethane groups. In the
221 spectrum of sample CU4, the relatively higher intensity of the band at 1015 cm^{-1} , corresponding to C-O
222 stretching vibration of alcohol, indicates that hydrolysis had occurred [42]. However, the
223 spectroscopic results highlight the persistence of a significant portion of free amines (band at 3536
224 cm^{-1}).

225

226 **Table 2** Vibrational band assignment for the ATR-FTIR spectrum of sample CU3 (bulk) from “Contentitoreumano
 227 n.1”, shown in Figure 3.1 [19,38-42].

Wavenumber (cm^{-1})	Assignment
3661 - 3434	ν N-H (non H-bonded)
3293	ν N-H (H-bonded)
3016 - 3112	ν C-H (benzene ring)
2971	ν_a C-H ₃
2929	ν_a C-H ₂
2895	ν C-H
2868	ν_s C-H ₃
1726	ν O=C (urethane, non H-bonded) ν O=C (bidentate urea, ordered H-bonded)
1642	
1599	ν C=C (benzene ring)
1538, 1262	δ O=C-N-H ν O=C-N-H
1474	δ C-H ₂
1451	δ_a C-H ₃
1412	Trimer band (isocyanurate ring)
1373	δ_s C-H ₃
1343	ω C-H ₂
1296, 1225	ν C-N
1095	ν_s C-O-C (polyether-based polyol)
1015	ν C-O-H
927	ρ C-H ₃
868, 817, 770	ω C-H (benzene ring)
710, 673	δ C-H (benzene ring)

228

229 **Table 3** Vibrational band assignment for the ATR-FTIR spectrum of sample CU4 (surface) from
 230 “Contentitoreumano n.1”, shown in Figure 3.2 [19,38-42]

Wavenumber (cm^{-1})	Assignment
3536	ν N-H (non H-bonded)
3408 - 3376	ν O-H (H-bonded)
3293	ν N-H (H-bonded)
3121 - 3005	ν C-H (benzene ring)
2970	ν_a C-H ₃
2918	ν_a C-H ₂
2897	ν C-H
2871	ν_s C-H ₃
2865, 2852	ν_s C-H ₂
1723	ν O=C (urethane, non H-bonded) ν O=C (urethane, loosely associated through H-bonds)
1713	
1689	ν O=C (urea free)
1675	ν O=C (monodentate urea, disordered H-bonded)
1643	ν O=C (bidentate urea, ordered H-bonded)
1600	ν C=C (benzene ring)
1538, 1262	δ O=C-N-H ν O=C-N-H
1472, 1464	δ C-H ₂
1452	δ_a C-H ₃
1416	Trimer formation band (isocyanurate ring)
1373	ω C-H ₂

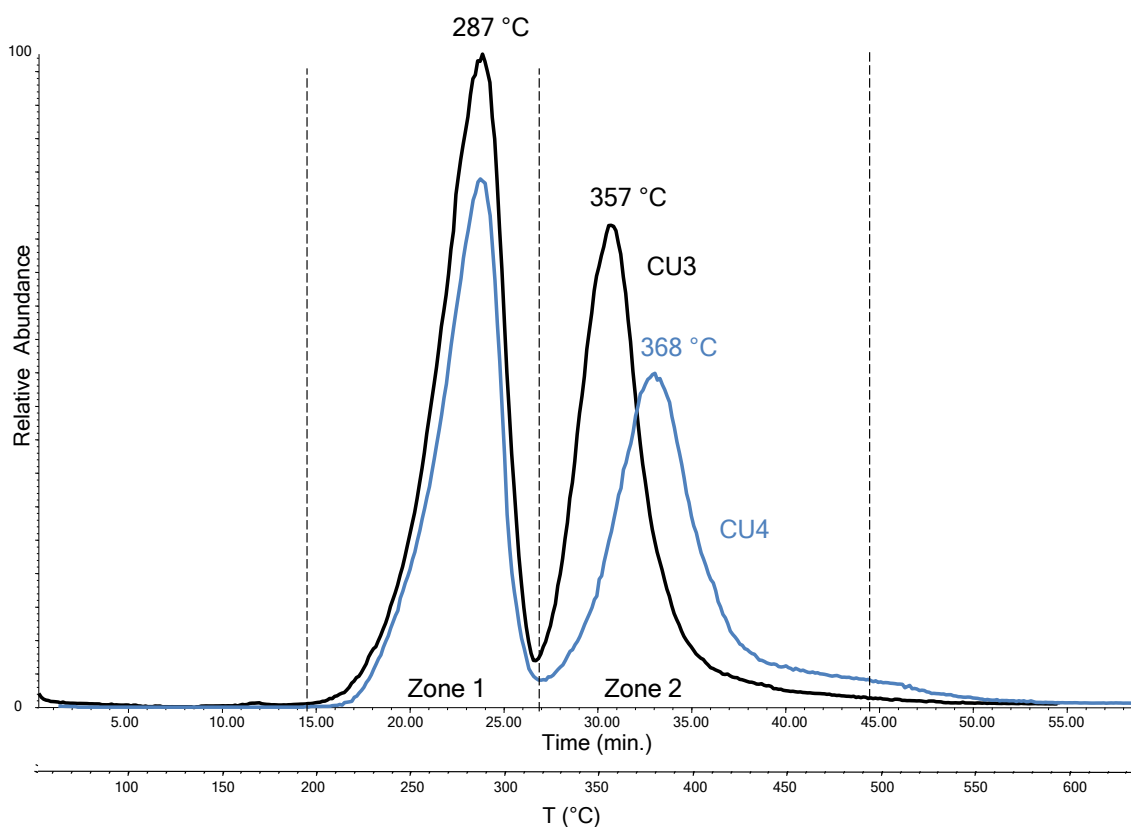
1344	δ_s C-H ₃
1297, 1225	ν C-N
1096	ν_a C-O-C (polyether-based polyol)
1017	ν C-O-H
927	ρ C-H ₃
870, 817	ω C-H (benzene ring)
758, 710, 668	δ C-H (benzene ring)

231

232

233 3.3 EGA-MS

234 Figure 4 shows the overlaid EGA-MS curves of the two samples from “Contentitoreumano n.1”. EGA-MS
 235 provides thermal degradation profiles and chemical information on the thermal decomposition
 236 products of PUs through their mass spectra [47].



237

238 **Figure 4** EGA-MS curves obtained for the bulk sample CU3 (black curve) and surface sample CU4 (blue curve)
 239 from “Contentitoreumano n.1”. The curve intensity was normalised for the weight of the samples.
 240

241 Two thermal decomposition zones were detected for the “Contentitoreumano n.1” PU foam: zone 1
 242 from 200 °C to 320 °C with a peak at 287 °C and zone 2 from 320 °C to 500 °C with a peak at 357 °C for
 243 sample CU3, and a peak at 368 °C for sample CU4. The first thermal degradation step is related to the
 244 desorption of additives and plasticizers and to the first step of the depolymerisation of polyurethane
 245 linkage in the temperature range 250-300 according to the literature [48], leading to isocyanate-
 246 terminated chains with diminished molar mass.

247 The most abundant ions in the mass spectra of this region were fragments with m/z 174, 148, 145,
248 132, 106, 77, 65, 51 which correspond to 2,6-toluenediisocyanate, and 149, 121, 132, 93 which
249 correspond to phthalates [49].

250 The second thermal degradation step is related to the complete pyrolysis of the polymeric network.
251 The most abundant ions in the mass spectra of the second thermal degradation zone in the mass
252 spectra were fragments with m/z 117, 101, 87, 73, 59 attributable to the fragmentation of polyether-
253 based polyols constituting the soft segments of PU, such as polypropylene glycol [50] of polyurethane.
254 Comparing the EGA profiles of the two samples, the first step thermal degradation temperature was
255 the same for both samples, while the EGA curve of sample CU4 showed a 50 °C increase in the
256 degradation temperature of the polymeric network. This may be caused by the cross-linking process
257 which leads to an increase in the hardness and brittleness of the foam.

258 Significant ions were extracted from the EGA profiles in order to compare the bulk sample CU3 and
259 surface sample CU4 (Figure 5).

260 The fragmentograms of these significant ions were compared for the two samples: ions with m/z 149
261 which corresponds to phthalates, m/z 148 which corresponds to a toluene diisocyanate (TDI) with one
262 isocyanate group replaced by an amino group, and m/z 59, an oligomer of polyether-based polyol.
263 From the extracted ion thermograms, the main difference between the two samples was a reduction in
264 the amount and type of phthalates (m/z 149) in the surface sample (CU4). This could indicate that
265 degradation leads to a loss in the volatile component of additives.

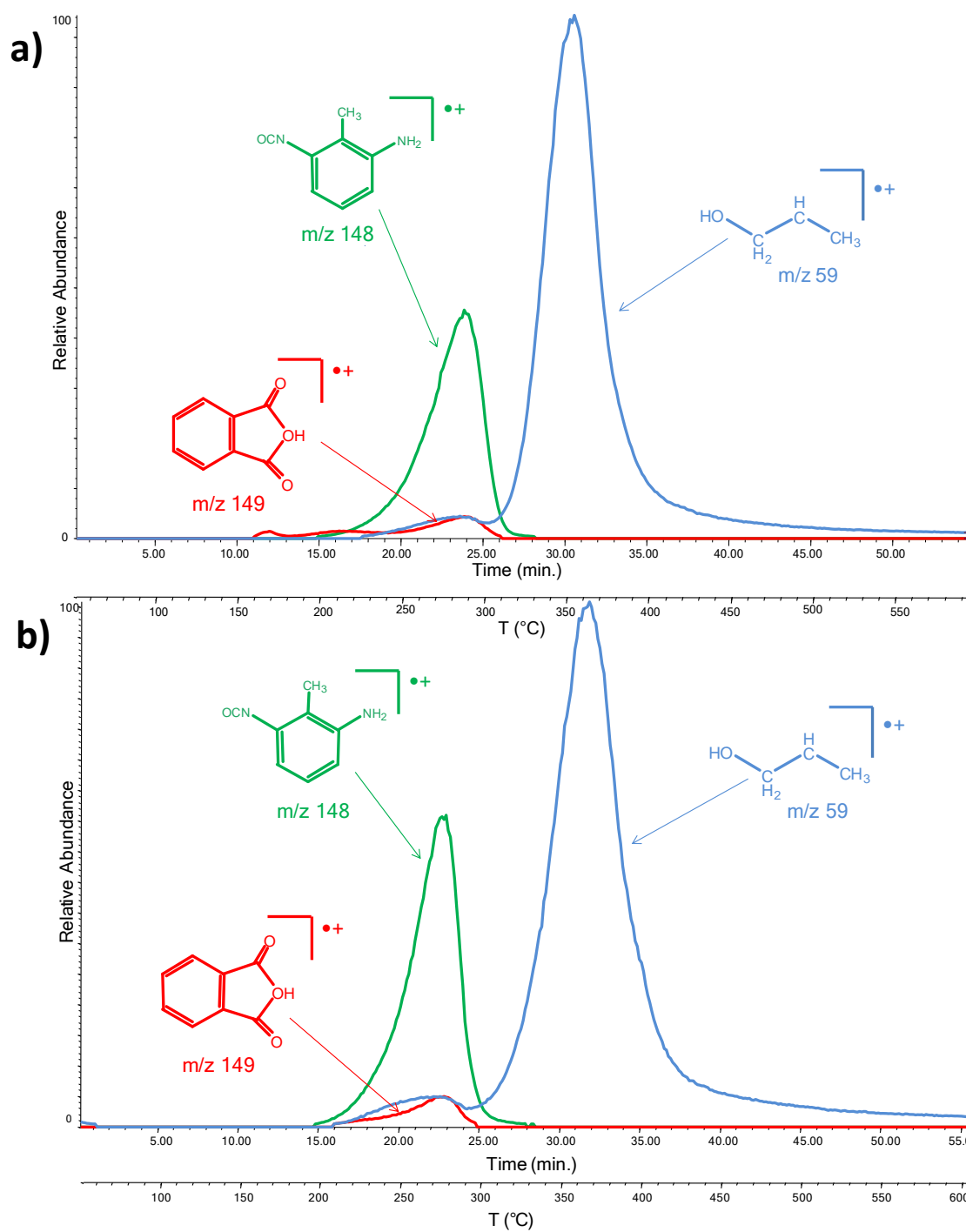
266 In particular, in the degraded sample CU4 the contribution of isocyanate with one isocyanate group
267 replaced by an amino group (ion m/z 148) was relatively higher than in CU3, when compared to the
268 intensity of the polyols fragments (ion m/z 59).

269 Interpreting the EGA-MS results together with the FTIR-ATR results we can hypothesize that the
270 photooxidation caused more pronounced changes in the soft segments of PU, leading to the
271 volatilization of low molecular weight products, suggested by the decreased intensity of the
272 absorption band at 1096 cm⁻¹ in the CU4 sample, and higher contribution of isocyanate derivatives in
273 the volatile compounds, indicating a decreased ratio of the soft to hard segments as a result of 50 years
274 of ageing, which has induced an higher concentration of NH substituted terminal groups in the
275 pyrolysis products (as confirmed by the appearance of the FTIR band at 3536 cm⁻¹ in the degraded
276 sample CU4).

277

278

279



280

281 Figure 5 Extracted ion (m/z 59, 148, and 149) thermograms of evolved gas during the thermal degradation
 282 obtained for the bulk sample CU3 (a) and surface sample CU4 (b) from "Contentitoreumano n.1"

283

284

285

286

287

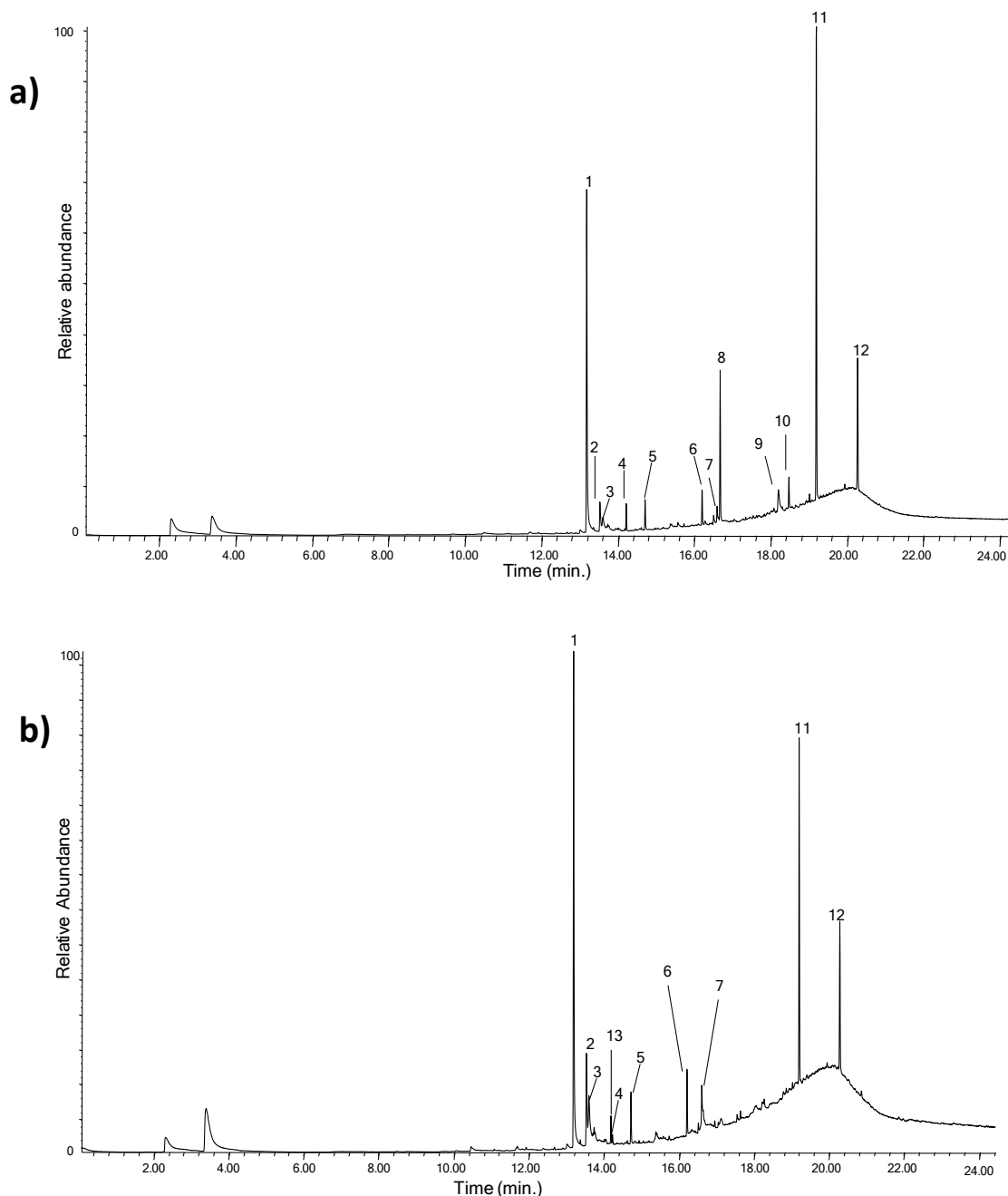
288

289 **3.4 Py-GC/MS**

290 Double-shot pyrolysis temperatures for the Py-GC/MS analysis of “Contentitoreumano n.1” were
291 selected on the basis of the EGA profiles. The temperatures for the two steps (306 °C and 600 °C) were
292 selected at the end of the EGA-MS bands (Figure 4) in order to collect all the evolved products.

293 Figure 6 shows first-shot pyrograms at 306°C of the bulk sample CU3 and the surface sample CU4,
294 respectively. The peak identification is reported in Table 4.

295



296

297 Figure 6 Py-GC/MS chromatogram obtained after first-shot pyrolysis at 306 °C of a) sample CU3 (bulk PU foam)
298 and b) sample CU4 (surface PU foam) from “Contentitoreumano n.1”. Peak identification is reported in Table 4.

299

300 In the first-shot pyrogram of both samples, the most abundant species are free 2,6-
301 diisocyanatetoluene (n°1) [29,51] (identified as the precursor used in the synthesis of the

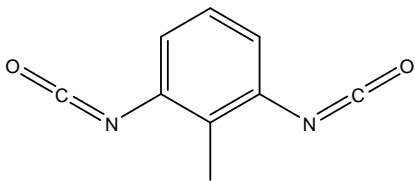
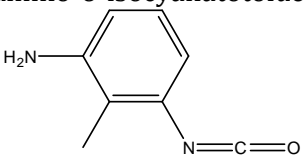
302 polyurethane foam), its rearrangement products 2-amino-6-isocyanatotoluene (n° 2,3) [28], and
 303 phthalic acid esters (n° 5, 6, 8, 10, 11).

304 Phthalates are the most widely used plasticizers in the synthesis of polyurethane, and account for 92%
 305 of all plasticizers[52]. The main differences highlighted from the comparison of the pyrograms of the
 306 two samples were: the change in the relative abundance of the isocyanate peak (n° 1) and the
 307 reduction in the amount and type of phthalates (loss of di-n-butyl phthalate and butyl benzyl
 308 phthalate) in the surface sample CU4. These changes are in agreement with the EGA information.

309
 310

311 **Table 4** Identification of chromatographic peaks in the first-shot (306 °C) pyrograms of samples CU3 and CU4
 312 from “Contentoreumano n.1” shown in Figure 6.

313
 314

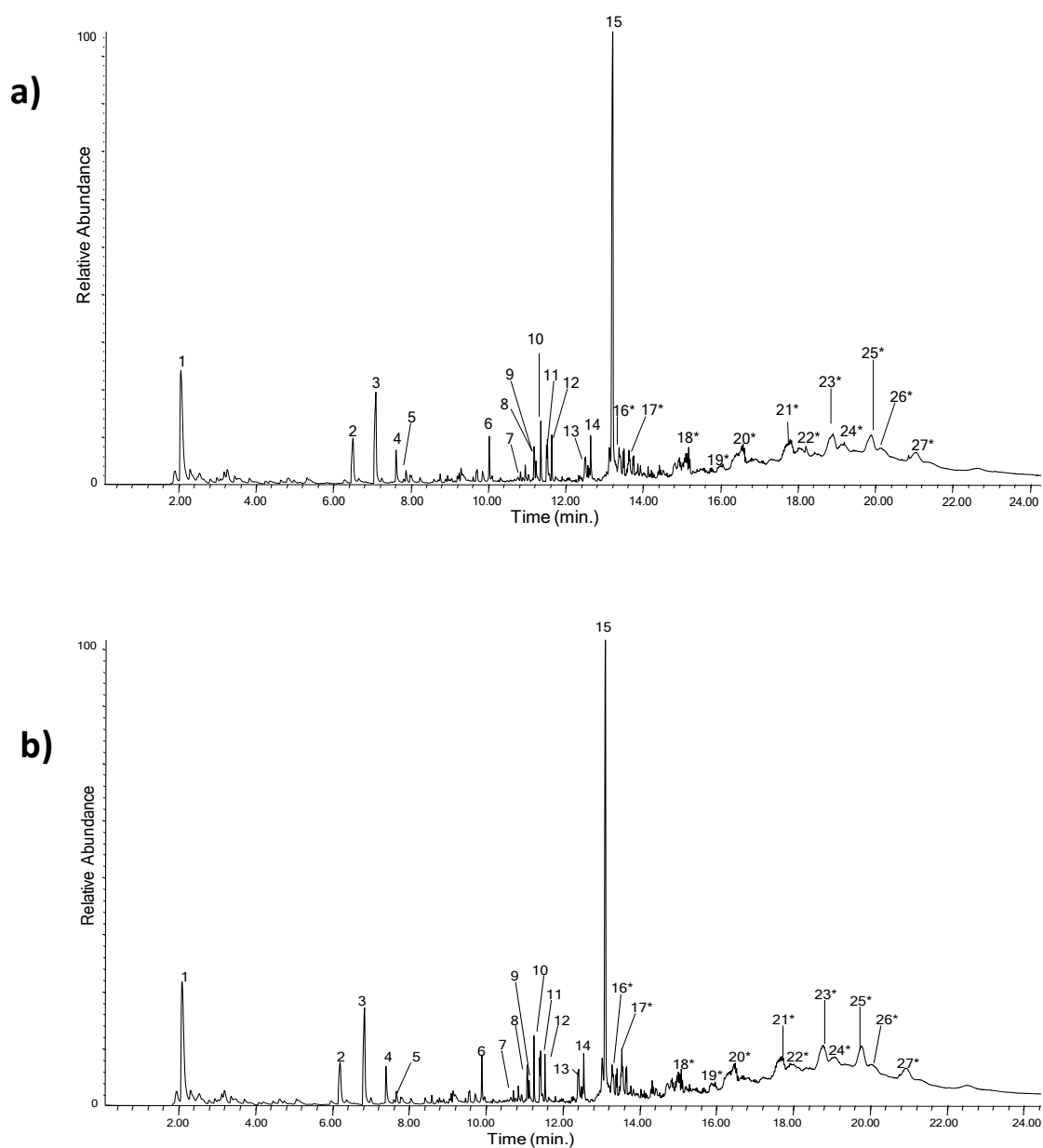
Peak number	Peak identification	Main ions (m/z)
	2,6-diisocyanatotoluene	
1		174,145, 132, 118, 91
	2-amino-6-isocyanatotoluene	
2		148, 120, 106, 93, 77, 65, 52
3	2-amino-6-isocyanatotoluene (<i>isomer</i>)	148, 119, 106, 93, 77, 65,51
4	4-methyl-2,6-di-tert-butylphenol	220, 205, 145, 57
5	Diethylphthalate	177, 149, 105, 93, 76, 65
6	Di-isobutylphthalate	223, 149, 104, 76, 57
7	Hexadecanoic acid	256, 213, 129, 115, 73, 60
8	Di-n-butylphthalate	223, 205, 149, 104, 76
9	2-cyclohexen-1,4-diol	105, 96, 70
10	Butylbenzylphthalate	312, 238, 206, 149, 104, 91, 65
11	Bis(2-ethylhexyl) phthalate	279, 167, 149, 113, 93, 83, 71, 57
12	Squalene	410, 148, 137, 121, 109, 95, 81
13	2,4-di-tert-butylphenol	206, 191, 91, 74, 57

315
 316

317 Figure 7 shows second-shot pyrograms at 600 °C of the bulk sample CU3 and the surface sample CU4,
 318 respectively. The peak identification is reported in Table 5.

319 In the time range of 0-10 minutes, the main pyrolysis products derived from chain extenders and
 320 cross-linkers such as n-butane, diethylamine and butanamide. Between 10 and 13 minutes 2,6-

321 diisocyanatotoluene (n° 15) and its rearranged molecule (n° 7), and derivatives of propylic alcohol,
322 derived from the polymeric network were observed. A cluster corresponding to different chain length
323 ether oligomers (m/z 174, 148, 117, 101, 87, 73, 59) was observed in the time range of 13-22 minutes.
324 The polyether-based polyol used in the synthesis of this PU foam was found to be polypropylene glycol
325 [28] from the analysis of the mass spectra (m/z 117, 87, 73, 59).
326 A comparison of the pyrograms at 600 °C of the samples from “Contentitoreumano n.1” did not show
327 significant differences between the two samples. The higher decomposition temperature observed in
328 the EGA profile of sample CU4 was not associated with a different qualitative and quantitative profile
329 of pyrolysis products. This is concurring with the occurrence of crosslinking.



330

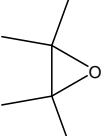
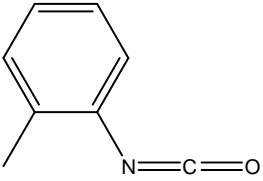
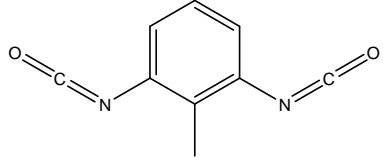
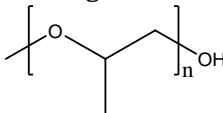
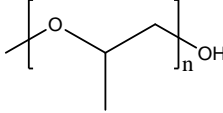
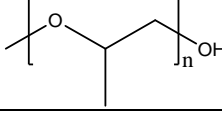
331 Figure 7 Py-GC/MS chromatogram obtained after second-shot pyrolysis at 600 °C of a) sample CU3 (bulk PU
332 foam) and b) sample CU4 (surface PU foam) from “Contentitoreumano n.1”. Peak identification is reported in
333 Table 5.

334

335

336
337
338

Table 5 Identification of chromatographic peaks in the second-shot (600 °C) pyrograms of samples CU3 and CU4 from "Contentitoreumano n.1" shown in Figure 7.

Peak number	Peak identification	Main ions (m/z)
1	n-butane	58
2	n-ethyl acetamide	87
3	Diethylamine	73, 58
4	Propyleneoxide	58
5	Butanamide	87, 72, 59
	Tetramethyloxirane	
6	 1-isocyanate-2-methylbenzene	100, 59
7		133, 104, 91, 78
8	3-(3-isopropoxy)propoxy-propanol	145, 117, 103, 87, 73, 59
9	1-(2-allyloxy-1-methylethoxy)-2-propanol	103, 85, 73, 59
10	Unknown	131, 114, 101, 89, 73, 59
11	Propyleneglycol trimer	117, 103, 73, 59
12	Unknown	114, 101, 84, 71, 57
13	Propyleneglycol trimer	117, 103, 87, 73, 59
14	1-(1-methylpropoxy)-butane 2,6-diisocyanatotoluene	115, 101, 83, 73, 57
15		174, 145, 132, 118, 103, 91
	Oligomers	
16*		117, 87, 73, 59
	Oligomers	
17-20*		148, 117, 101, 87, 72, 59
	Oligomers	
21-27*		174, 148, 115, 101, 87, 73, 59

339 * cluster from 13.3 min to 21.6 min

340

341

342 **4. Conclusions**

343 Our multi-analytical approach based on the use of infrared spectroscopy and two different analytical
344 pyrolysis methodologies, double shot Py-GC/MS and EGA-MS, was successfully applied in the study of
345 the polyurethane artwork “Contentitoreumano n.1” (1968). The integrated interpretation of the results
346 obtained with the three analytical methods enabled us to obtain a detailed picture of the composition
347 and the state of preservation of the PU material used to produce the object. The isocyanate and polyol
348 precursors, as well as the plasticizers, used in the production of the PU foam were identified by mass
349 spectrometry. Different aspects of the degradation processes undergone by the surface portion of the
350 foam were also highlighted by the three techniques, on the basis of a comparison with a sample of
351 better preserved foam from the bulk:

- 352 - ATR-FTIR analysis revealed a combination of hydrolysis, reticulation, and photo-oxidative
353 processes;
- 354 - EGA-MS highlighted an increase in the thermal degradation temperature of the polymer due to
355 to crosslinking;
- 356 - double shot Py-GC/MS revealed the loss of plasticizers.

357 The application of EGA-MS and multi-shot Py-GC/MS in investigating synthetic polymer-based plastics
358 in artworks and design objects appears extremely promising for future heritage studies and is worth
359 extending to a wider range of materials and objects. When compared to conventional flash-pyrolysis
360 coupled with GC/MS, EGA-MS and multi-shot Py-GC/MS extend the pyrolysis analyses of polymers
361 beyond a mere identification or classification. These methods could achieve selectivity in the
362 investigation of specific fractions and provide semi-quantitative information, such as partial cross-
363 linking and loss of plasticizers, which could be successfully exploited to compare samples in different
364 states of preservation.

365 According to these analytical results, the macroscopic appearance and brittleness of the degraded
366 portion of the PU foam could be related to parallel processes of photolysis and hydrolysis, together
367 with a partial reticulation and cross-linking involving the hydrolyzed portion of the PU foam. In detail,
368 photooxidation of polyether-based PUs component lead to molecular mass degradation accompanied
369 by crosslinking that could be considered as prevailing mechanisms in soft segments ageing.

370 The surface in fact showed a lower elasticity than the internal part of the object. The loss of plasticizers
371 leads to a further worsening of the physical properties, leading to fragmentation and loss of foam
372 flakes.

373 On the basis of the results of the investigation performed on “Contentitoreumano n.1”, the Triennale
374 Design Museum Conservation Department decided to plan a restoration, which included a dry-
375 cleaning protocol and gluing of the layers. Consolidation was considered but not carried out at this
376 stage due to the fairly good condition of the bulk of the foam [31].

377

378

379

380

381 **Acknowledgments**

382 The authors would like to thank Silvana Annicchiarico, Director of the Triennale Design Museum
383 (Milan), and Rafaela Trevisan of the Conservation Laboratory of the Museum for their essential
384 contribution in the investigation of “Contenitoreumano n.1”. The research was funded by the IPERION-
385 CH.it Platform as part of the ALRTDM Project “Plastic materials in the Collection of Triennale Design
386 Museum in Milan”, and by the University of Pisa as part of the PRA_2016_13 Project "Analytical
387 chemistry for the knowledge of materials and techniques in modern and contemporary art”. The
388 authors also acknowledge three anonymous reviewers for useful comments and suggestions.

389

390 **REFERENCES**

- 391 [1] T.v. Oosten, Y. Shashoua, F. Waentig, K. Fachhochschule, K. Fachbereich Restaurierung und
392 Konservierung von Kunst- und, I.C.f. Conservation and G. Modern Materials Working, *Plastics in art*
393 *: history, technology, preservation*, München, 2002.
- 394 [2] Y. Shashoua, *Conservation of plastics : materials science, degradation and preservation*, 2016.
- 395 [3] I. Degano, F. Modugno, I. Bonaduce, E. Ribechini and M.P. Colombini, *Angewandte Chemie Int. Ed.*,
396 in press, (2018).
- 397 [4] E. Ghelardi, I. Degano, M.P. Colombini, J. Mazurek, M. Schilling, H. Khanjian and T. Learner, *Dyes*
398 *and Pigments*, 123, (2015) 396.
- 399 [5] A. Heginbotham and M. Schilling, *East Asian Lacquer: Material Culture, Science and Conservation*.
400 *London: Archetype*, (2011) 92.
- 401 [6] D. Scalarone and O. Chiantore, *Journal of separation science*, 27, (2004) 263.
- 402 [7] J. La Nasa, S. Orsini, I. Degano, A. Rava, F. Modugno and M.P. Colombini, *Microchemical Journal*,
403 124, (2016) 940.
- 404 [8] S. Carlesi, G. Bartolozzi, C. Cucci, V. Marchiafava, M. Picollo, J. La Nasa, F. Di Girolamo, M. Dilillo, F.
405 Modugno and I. Degano, *Spectrochimica Acta Part A: Molecular and Biomolecular Spectroscopy*,
406 168, (2016) 52.
- 407 [9] G. Bartolozzi, C. Cucci, V. Marchiafava, S. Masi, M. Picollo, E. Grifoni, S. Legnaioli, G. Lorenzetti, S.
408 Pagnotta and V. Palleschi, *Heritage Science*, 2, (2014) 29.
- 409 [10] A. Lattuati-Derieux, S. Thao-Heu and B. Lavédrine, *Journal of Chromatography A*, 1218, (2011) 4498.
- 410 [11] S. Wei, V. Pintus and M. Schreiner, *Journal of analytical and applied pyrolysis*, 97, (2012) 158.
- 411 [12] S. Wei, V. Pintus and M. Schreiner, *Journal of analytical and applied pyrolysis*, 104, (2013) 441.
- 412 [13] I. Bonaduce, M.P. Colombini, I. Degano, F. Di Girolamo, J. La Nasa, F. Modugno and S. Orsini,
413 *Analytical and Bioanalytical Chemistry*, 405, (2013) 1047.
- 414 [14] R. Ploeger, D. Scalarone and O. Chiantore, *Journal of Cultural Heritage*, 9, (2008) 412.
- 415 [15] D. Tamburini, J.J. Łucejko, E. Ribechini and M.P. Colombini, *Journal of Mass Spectrometry*, 50,
416 (2015) 1103.
- 417 [16] D. Tamburini, J.J. Łucejko, F. Modugno and M.P. Colombini, *Journal of Analytical and Applied*
418 *Pyrolysis*, 122, (2016) 429.
- 419 [17] N. Niimura, *Thermochimica Acta*, 532, (2012) 164.
- 420 [18] S. Orsini, F. Parlanti and I. Bonaduce, *Journal of Analytical and Applied Pyrolysis*, 124, (2017) 643.
- 421 [19] F. de Sà, J. L. Ferreira, I. Pombo Cardoso, R. Macedo and A. M. Ramos, *Polymer Degradation and*
422 *Stability*, 144, (2017) 354.
- 423 [20] T. van Oosten, *Pur Facts Conservation of Polyurethane Foam in Art and Design*, Amsterdam
424 University Press, 2011.
- 425 [21] T. van Oosten, Y. Shashoua and F. Waentig, *Plastics in Art : History, Technology, Preservation*, Siegl,
426 2002.
- 427 [22] G. Mitchell, F. France, A. Nordon, P.L. Tang and L.T. Gibson, *Heritage Science*, 1, (2013) 28.
- 428 [23] C. Morales Muñoz, *Applied Surface Science*, 256, (2010) 3567.
- 429 [24] M. Lazzari, A. Ledo-Suárez, T. López, D. Scalarone and M.A. López-Quintela, *Analytical and*
430 *Bioanalytical Chemistry*, 399, (2011) 2939.
- 431 [25] M. Manfredi, E. Barberis, A. Rava, T. Poli, O. Chiantore and E. Marengo, *Analytical and Bioanalytical*
432 *Chemistry*, 408, (2016) 5711.
- 433 [26] M. Manfredi, E. Barberis and E. Marengo, *Applied Physics A*, 123, (2016) 35.
- 434 [27] E. Pellizzi, A. Lattuati-Derieux, B. Lavédrine and H. Cheradame, *Polymer Degradation and Stability*,
435 107, (2014) 255.
- 436 [28] G.L. Marshall, *European Polymer Journal*, 19, (1983) 439.
- 437 [29] S. Tsuge, H. Ohtani and C. Watanabe, *Pyrolysis-GC/MS data book of synthetic polymers*, Elsevier
438 Science, 2011.
- 439 [30] B.-H. Kim, K. Yoon and D.C. Moon, *Journal of Analytical and Applied Pyrolysis*, 98, (2012) 236.

- 440 [31] S. Annichiarico, B. Ferriani, R. Trevisan, J.L. Nasa, F. Modugno and M.P. Colombini, *Bringin back to*
441 *life the Contenitoreumano* at: FUTURE TALKS 017 -The silver edition- Visions. Innovation in
442 technology and conservation of the modern, Munich, In press,
- 443 [32] S. Carlesi, M. Ricci, C. Cucci, J.L. Nasa, C. Lofrumento, M. Picollo and M. Becucci, *Applied*
444 *Spectroscopy*, 69, (2015) 865.
- 445 [33] M. Faraco, D. Fico, A. Pennetta and G.E. De Benedetto, *Talanta*, 159, (2016) 40.
- 446 [34] S. Orsini, J. La Nasa, F. Modugno and M. Colombini, *Journal of analytical and applied pyrolysis*, 104,
447 (2013) 218.
- 448 [35] J. La Nasa, F. Di Marco, L. Bernazzani, C. Duce, A. Spepi, V. Ubaldi, I. Degano, S. Orsini, S. Legnaioli
449 and M. Tiné, *Polymer Degradation and Stability*, 144, (2017) 508.
- 450 [36] J. La Nasa, M. Zanaboni, D. Uldanck, I. Degano, F. Modugno, H. Kutzke, E.S. Tveit, B. Topalova-
451 Casadiego and M.P. Colombini, *Analytica Chimica Acta*, 896, (2015) 177.
- 452 [37] G. Wypych, *Handbook of Material Weathering*, ChemTec Pub., 2013.
- 453 [38] I. Yilgör, E. Yilgör and G.L. Wilkes, *Polymer*, 58, (2015) 1.
- 454 [39] R. D. Priester, J. V. McClusky, R. E. O'Neill, R. B. Turner, M. A. Hartcock and B.L. Davis, *Journal of*
455 *Cellular Plastics*, 26, (1990) 346.
- 456 [40] R. M. Silverstein, F. X. Webster and D. J. Kiemle, in *Spectrometric Identification of Organic*
457 *Compounds*, John Wiley and Sons Ltd, 2005, Chapter 2, p. 72.
- 458 [41] Z. Lan, R. Daga, R. Whitehouse, S. McCarthy and D. Schmidt, *Polymer*, 55, (2014) 2635.
- 459 [42] P. Davies and G. Evrard, *Polymer Degradation and Stability*, 92, (2007) 1455.
- 460 [43] M. M. Coleman, D. J. Skrovanek, J. Hu and P.C. Painter, *Macromolecules*, 21, (1988) 59.
- 461 [44] O. Thomas, R.D.P. Jr., K. J. Hinze and D. D. Latham, *Journal of Polymer Science Part B: Polymer*
462 *Physics*, 32, (1994) 2155.
- 463 [45] C. Wilhelm, A. Rivaton and J. Gardette, *Polymer*, 39, (1998) 1223.
- 464 [46] D. Rosu, L. Rosu and C.N. Cascaval, *Polymer Degradation and Stability*, 94, (2009) 591.
- 465 [47] B. Kim, K. Yoon and D. C. Moon, *Journal of Analytical and Applied Pyrolysis*, 98, (2012) 236.
- 466 [48] D. Allan, J. Daly and J.J. Liggat, *Polymer Degradation and Stability*, 98, (2013) 535.
- 467 [49] P. Yin, H. Chen, X. Liu, Q. Wang and R. Pan, *Analytical Letters*, 47, (2014) 1579.
- 468 [50] G. M. Neumann, P. G. Cullis and P.J. Derrick, *Zeitschrift für Naturforschung A*, 35, (1980) 1090.
- 469 [51] H. Ohtani, T. Kimura, K. Okamoto and S. Tsuge, *Journal of Analytical and Applied Pyrolysis*, 12,
470 (1987) 115.
- 471 [52] J. Murphy, in *Additives for plastics handbook*, ed. Elsevier Science, 2001, p. 169.

472